J Mol Model (2012) 18:4397–4408
DOI 10.1007/s00894-012-1435-y

ORIGINAL PAPER

Lead compound design for TPR/COX dual inhibition

Abhay Krishna · Arpita Yadav

Received: 2 February 2012 / Accepted: 17 April 2012 / Published online: 16 May 2012

Abstract The modes of action of TxA2 antagonists and COX-2 inhibitors were studied utilizing flexible ligand docking with postdocking minimization and ab initio interaction energy calculations. The resulting increased understanding of their binding interactions led to the design of a lead compound with chemical moieties that allowed efficient binding to both the thromboxane receptor and the COX-2 enzyme. This compound is derived from allicin, a natural component of garlic, and is a good starting point for the development of anti-inflammatory drugs with fewer side effects or improved cardiovascular drugs.

Keywords TxA2, dual inhibitor · TPR/COX · Synergistic · Allicin · Balanced dual inhibition · Cardiovascular

Introduction

Instances of mechanical stress, injury, trauma, and some immunological responses induce the release of arachidonic acid (AA) from membrane phospholipids in our body. AA triggers a number of transformations leading to the synthesis of various prostaglandins and eventually inflammation and pain at the site of action [1]. AA is first metabolized to prostaglandin H (PGH_2). This step is catalyzed by PGH synthase, also known as cyclooxygenase. Cyclooxygenase (COX) exists in two isoforms, COX 1 and COX 2, which perform similar enzymatic activities. COX 1 is constitutively expressed in many tissues including the GI tract, kidney, and platelets, whereas the expression of COX 2 is induced in response to inflammatory stimuli [2]. Both catalyze the formation of various prostaglandins. COX 1 catalyzes the synthesis of "good" prostaglandins involved in gastric cytoprotection and hemostatic integrity. COX 2 catalyzes the synthesis of "bad" prostaglandins leading to inflammation and pain. Nonsteroidal anti-inflammatory drugs (NSAIDs) block the production of various prostaglandins by inhibiting both COX 1 and COX 2. Most of these drugs are associated with well-known side effects at the gastrointestinal level and sometimes also at the renal level [3]. The beneficial effects of these drugs are a result of COX 2 inhibition, and adverse side effects are due to the inhibition of COX 1. Second-generation NSAIDs were therefore developed as selective inhibitors of COX 2. These drugs quickly become popular due to their mild effects on the GI tract. However, it was also realized that long-term usage of second-generation NSAIDs leads to cardiovascular problems [4]. In this case, the production of prostaglandins through COX 2 is selectively blocked, but the pathway through COX 1 is still open, resulting in the production of TxA_2. This induces platelet aggregation, which in turn leads to thromboembolism and cardiovascular problems. To avoid these adverse effects of selective COX 2 inhibition, research efforts are underway to develop dual antagonism strategies [5, 6]. Figure 1 illustrates the production

A. Krishna (✉) · A. Yadav (✉)
Department of Chemistry, University Institute of Engineering and Technology, CSJM University,
Kanpur 208024, India
e-mail: abhaykrishna51@gmail.com
e-mail: arpitayadav@yahoo.co.in

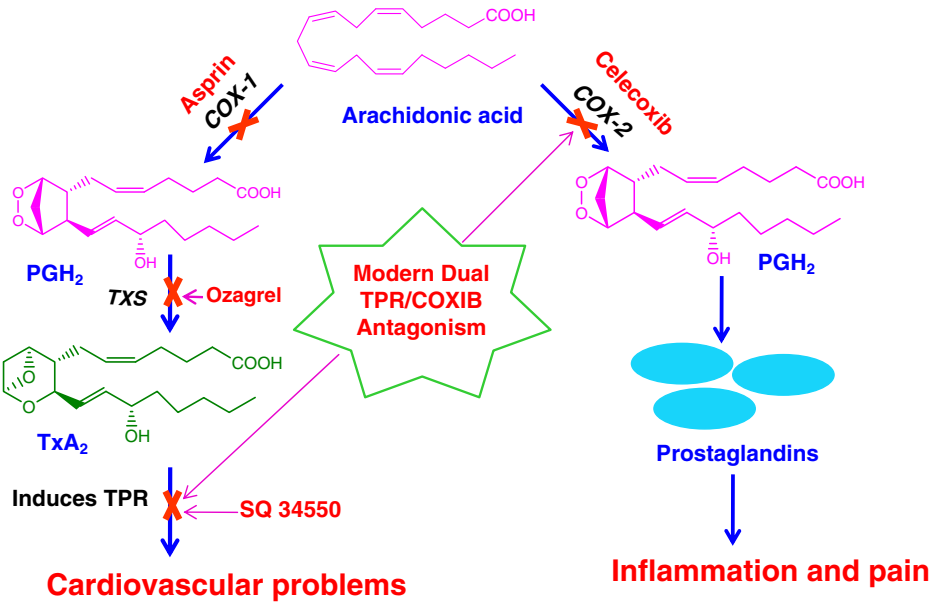

Fig. 1 Points of intervention during prostaglandin biosynthesis

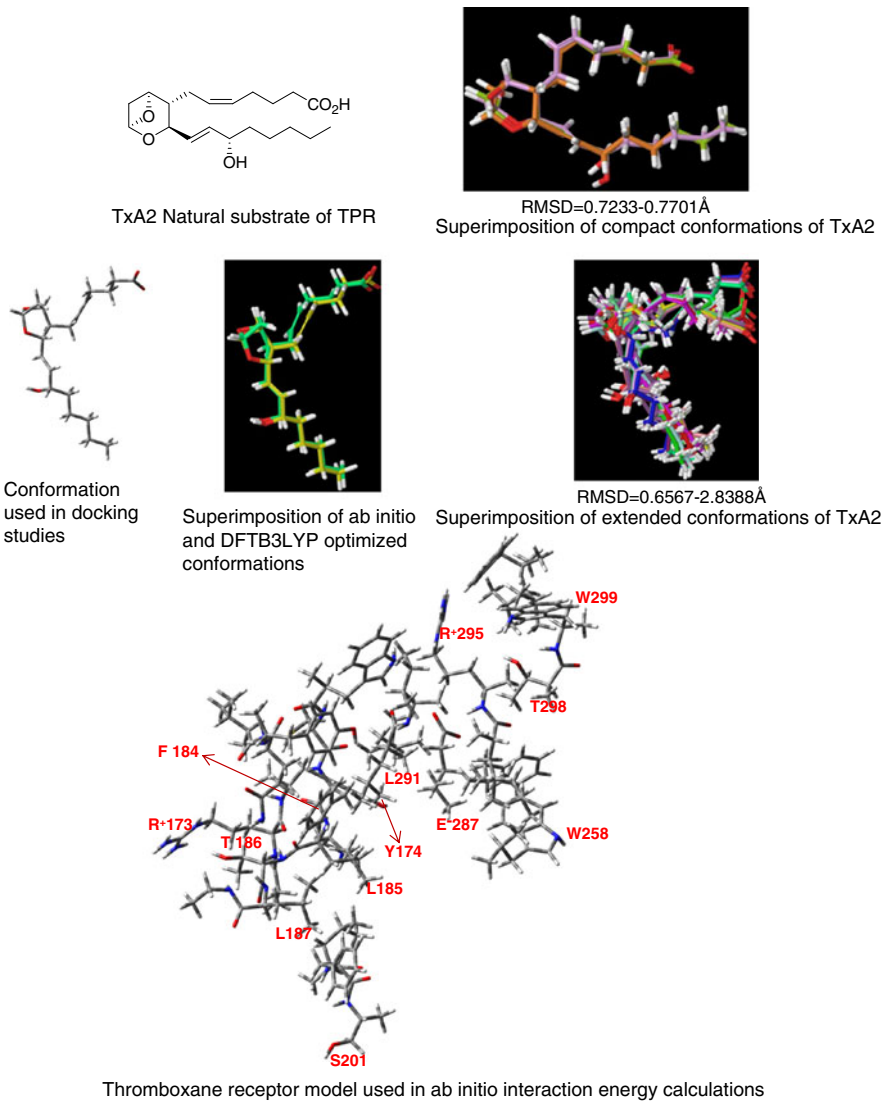

Fig. 2 Conformational mapping for TxA2 and the TPR model

of prostaglandins, points of intervention in the cycle, and the benefits of dual TP/COX inhibition.

In the study presented in this paper, we attempted the de novo design of dual COX/TP antagonists. The binding interactions of COX inhibitors with enzyme active-site residues and the binding interactions of TP antagonists with TPR binding-site residues were studied in detail. The resulting improved understanding of these binding interactions allowed us to design a dual TP/COX antagonist by blending pharmacophoric features of both antagonists.

Methodology

Ab initio quantum mechanical calculations with complete geometry optimization [7, 8] performed at the Hartree–Fock (HF) level and the DFTB3LYP level, utilizing the 6-31G* basis set [9, 10], were performed. Quantum mechanical calculations were coupled with docking studies and drug–receptor interaction energy calculations.

The following steps describe the procedure in detail.

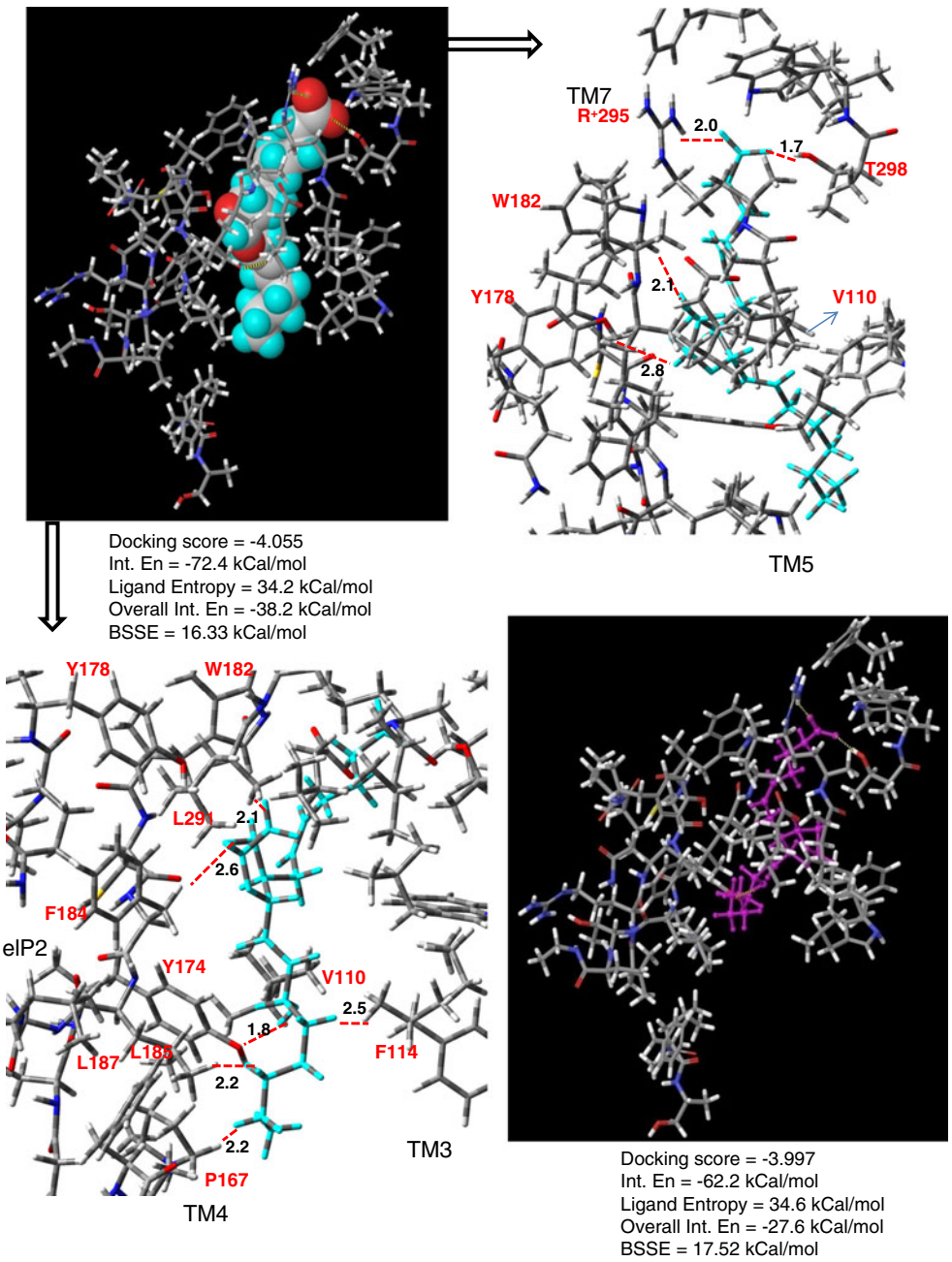

Fig. 3 Best two poses for the flexible ligand docking of TxA2 in the TPR. Results of ab initio interaction energy calculations are also shown. All distances are in Å

Ligand preparation

The geometries of selected TxA_2 agonists, antagonists, and COX-2 inhibitors were completely quantum-mechanically optimized using ab initio molecular orbital calculations. Experimental potency values were taken from [11–17]. Several conformations of each were prepared and energetically filtered for docking studies. A rough idea of possible bioactive conformations of ligands can be obtained by viewing the binding site of receptor and gauging the spatial constraints associated with it.

Receptor preparation

To prepare the model of the thromboxane receptor (TPR), the latest coordinates for human TPR available in SWISS PROT (entry P21731) [15–17] were obtained. This model lacks an important transmembrane segment containing residues that are involved in ligand binding. However, the complete model containing the desired transmembrane segment is available for the green monkey, so this model was taken to represent the human TPR model, considering the similarities between primates and humans. For ab initio calculations of the ligand–receptor interaction energies, 8 Å environment was taken throughout the length of inhibitor. Binding site residues are quite spread out in this case, and the inhibitors are very long, making modeling quite challenging. Similarly, to prepare a model of the COX-2 active site, the coordinates in the Brookhaven Protein Data Bank file 6COX [13, 14] were used. 8 Å environment around active site has been taken. In both cases, the ionizable residues were modeled in their respective ionized forms.

Docking and drug–receptor interaction energy evaluation

The ligands were sequentially docked using the Glide flexible ligand docking program [18–20] with postdocking minimization. The complete receptor was used in the automated docking studies. A target grid was superposed on the binding site residues. One thousand poses were generated, and

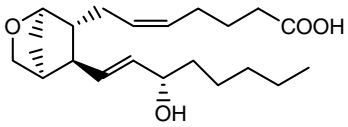

TPR agonist U44069
K_i 72.0 nM
EC_{50} 57.0 nM

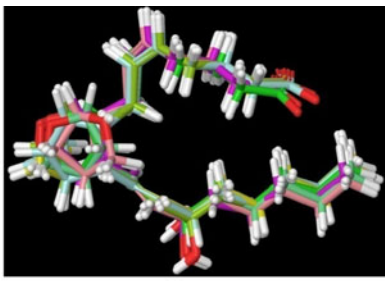

RMSD=0.611-1.609Å
Superimposition of compact conformations of U44069

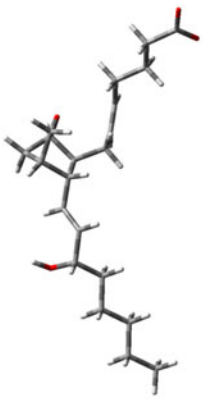

Conformation used in docking studies

Superimposition of ab initio and DFTB3LYP optimized conformations

RMSD=0.642-3.256Å
Superimposition of extended conformations of U64409

Fig. 4 Conformational mapping for the TPR agonist U44069

the best ten were selected to evaluate drug–receptor interaction energies using accurate supermolecule quantum mechanical calculations.

The interaction energies were calculated as:

$$E_{\text{interaction}} = E_{\text{complex}} - \left(E_{\text{drug}} + E_{\text{receptor}}\right). \quad (1)$$

Interaction energies were also corrected for basis set superposition error (BSSE). The BSSE was evaluated for all of the complexes, and all BSSE values were of a similar order of magnitude. Hence, comparisons can be made and inferences can be drawn.

Analysis and de novo design of a dual inhibitor

We used the ligand entropy changes and drug–receptor interaction energies to analyze the docking results. The analysis of drug–receptor interactions at COX and the TPR led to the design of a dual TP/COX inhibitor.

Results and discussion

Generating antagonistic activity at the thromboxane receptor (TPR) requires an understanding of the mode of action of the natural substrate TxA2 at the TPR. Therefore, we gen-

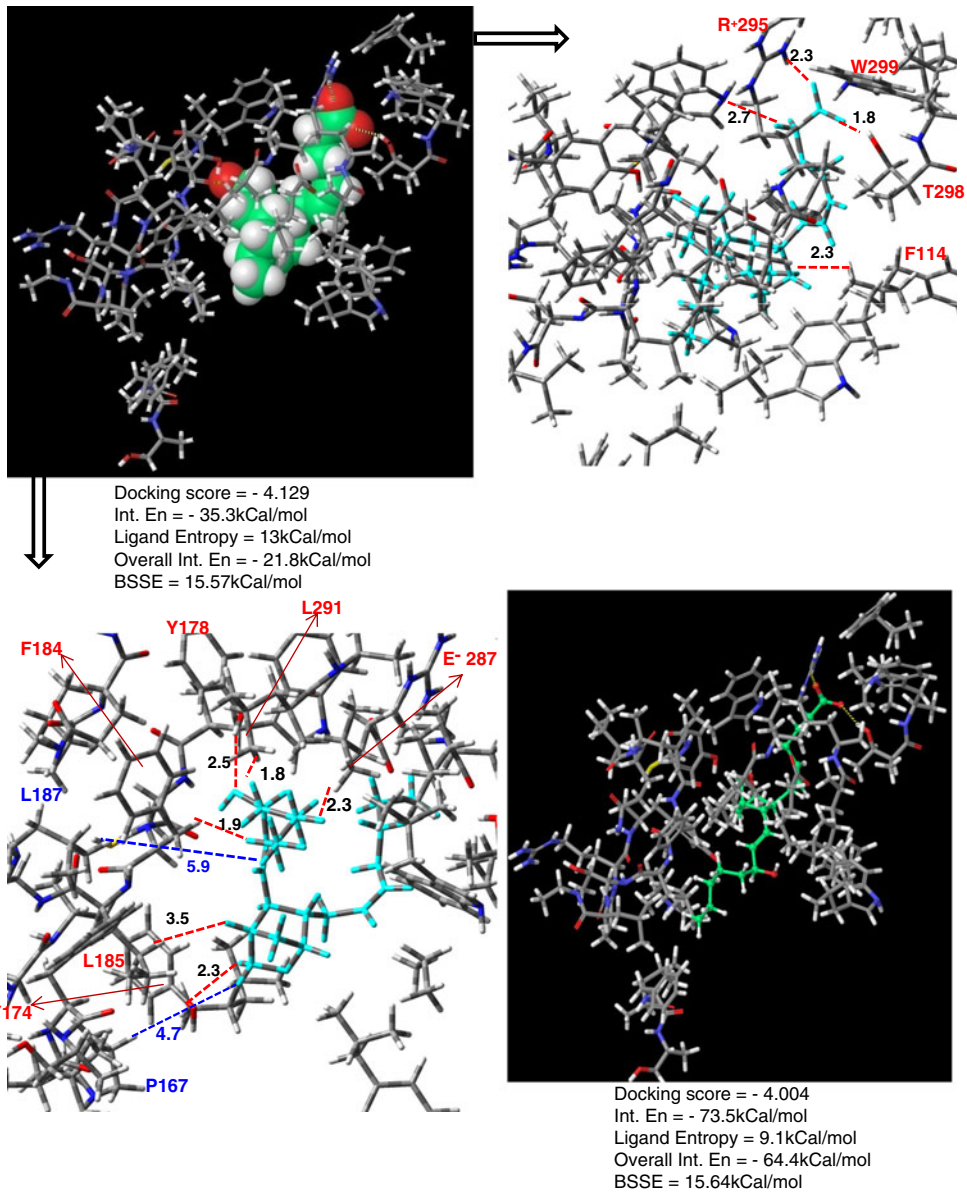

Fig. 5 Best two poses for the flexible ligand docking of U44069 in the TPR. Results of ab initio interaction energy calculations are also shown. Distances are in Å

erated different conformations of TxA2. Conformational mapping of these conformations, shown in Fig. 2, indicates that TxA2 most probably occurs as an extended conformation. The TPR model used for ab initio interaction energy calculations is shown in Fig. 2. TxA2 was first docked in the TPR using the GLIDE module of Maestro [21]. The results obtained from automated flexible ligand docking are shown in Fig. 3. Two zoomed-in figures are provided to highlight important interactions with various transmembranes of the receptor. Hydrogen-bonding interactions with T298, $R^{+}295$, L291 of TM7; W182, Y178, F184, Y174 of elP2 as well as F114 of TM3 and P167 of TM4 can be clearly seen. These results are in accord with site-directed mutagenesis results, showing the importance of these residues in binding the ligand and activating the receptor [22–25].

Frames corresponding to the best docking scores were selected for accurate interaction energy evaluation. The change in the ligand conformational entropy required was calculated in each case. The overall interaction energy indicates the feasibility of receptor activation. Results from ab initio intermolecular interaction energy calculations are also shown in these figures. All of the poses highlight the importance of strong electrostatic interactions between the negative site on the ligand and $R^{+}295$. Most of the poses also show hydrogen-bonding interactions between hydroxyls on TxA2 and L291. Low docking score poses correspond to cyclic conformations of TxA2, which are not well suited to receptor activation. Next, we studied a well–known TPR agonist, U44069. The structure and conformations of this agonist are shown in Fig. 4. U44069 shows an equal

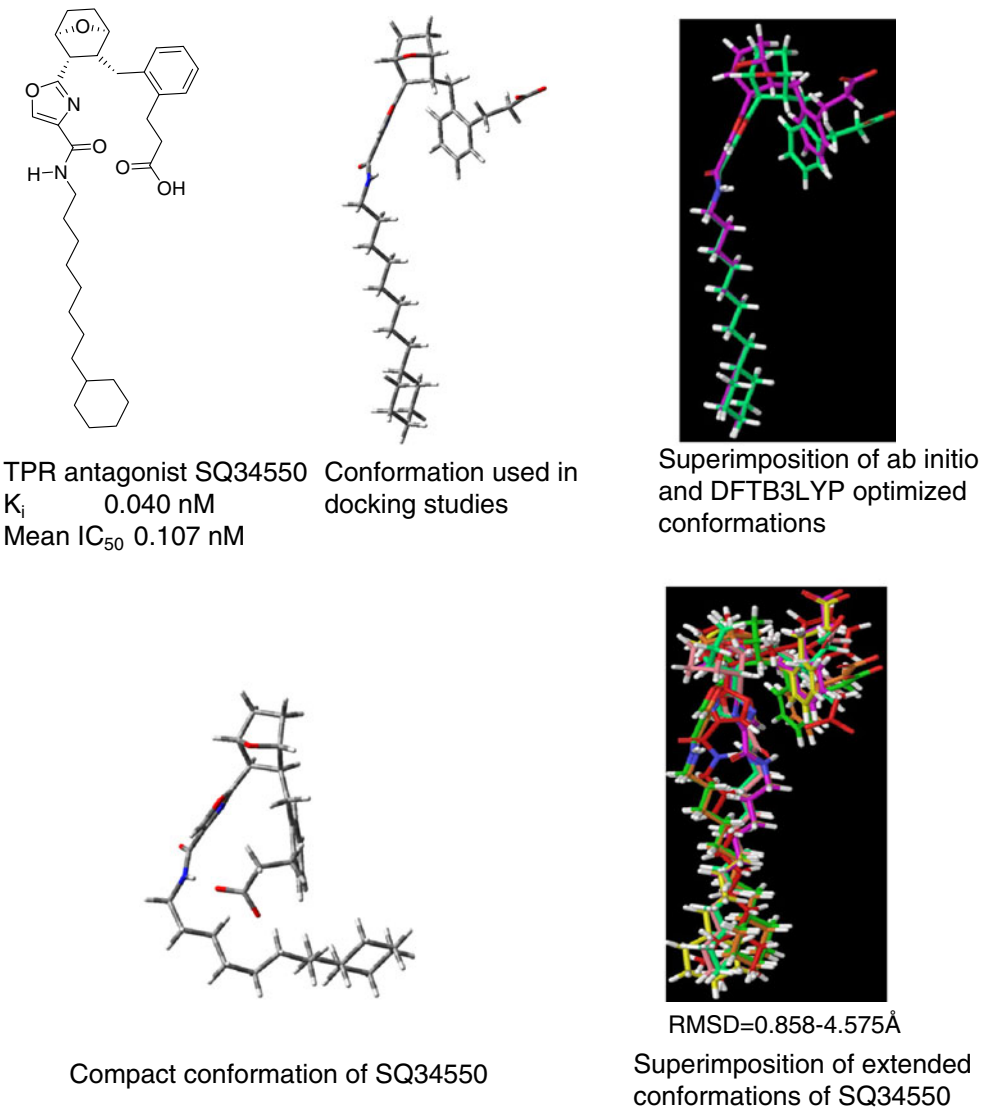

Fig. 6 Conformational mapping for the TPR antagonist SQ34550

probability of being cyclic or extended in conformation. Both conformations were considered in docking studies. The best docking results are shown in Fig. 5. Two poses corresponding to the best docking scores obtained are presented in blow-ups, which show various interactions. It is apparent that all interactions with TM7, TM3-4, and elP2 seen with the natural substrate TxA2 are maintained with U44069. The agonist shows enhanced interactions (involving $E^{-}287$) with elP2. The ligand conformational entropy is lower than for the natural substrate, suggesting that the agonist can act competitively.

To understand the difference between the mode of action of the natural substrate and an antagonist, we chose to study SQ34550, one of the many potent antagonists synthesized by Squibb pharmaceuticals [11]. The antagonist is conformationally locked in the vicinity of the negative site. A cyclohexyl ring at the end of the alkyl chain also restricts the conformational freedom of the compound, resulting in an extended conformation (see Fig. 6). The best poses for SQ34550, along with their docking scores and ab initio interaction energy calculations, are shown in Fig. 7. An S-shaped confor-

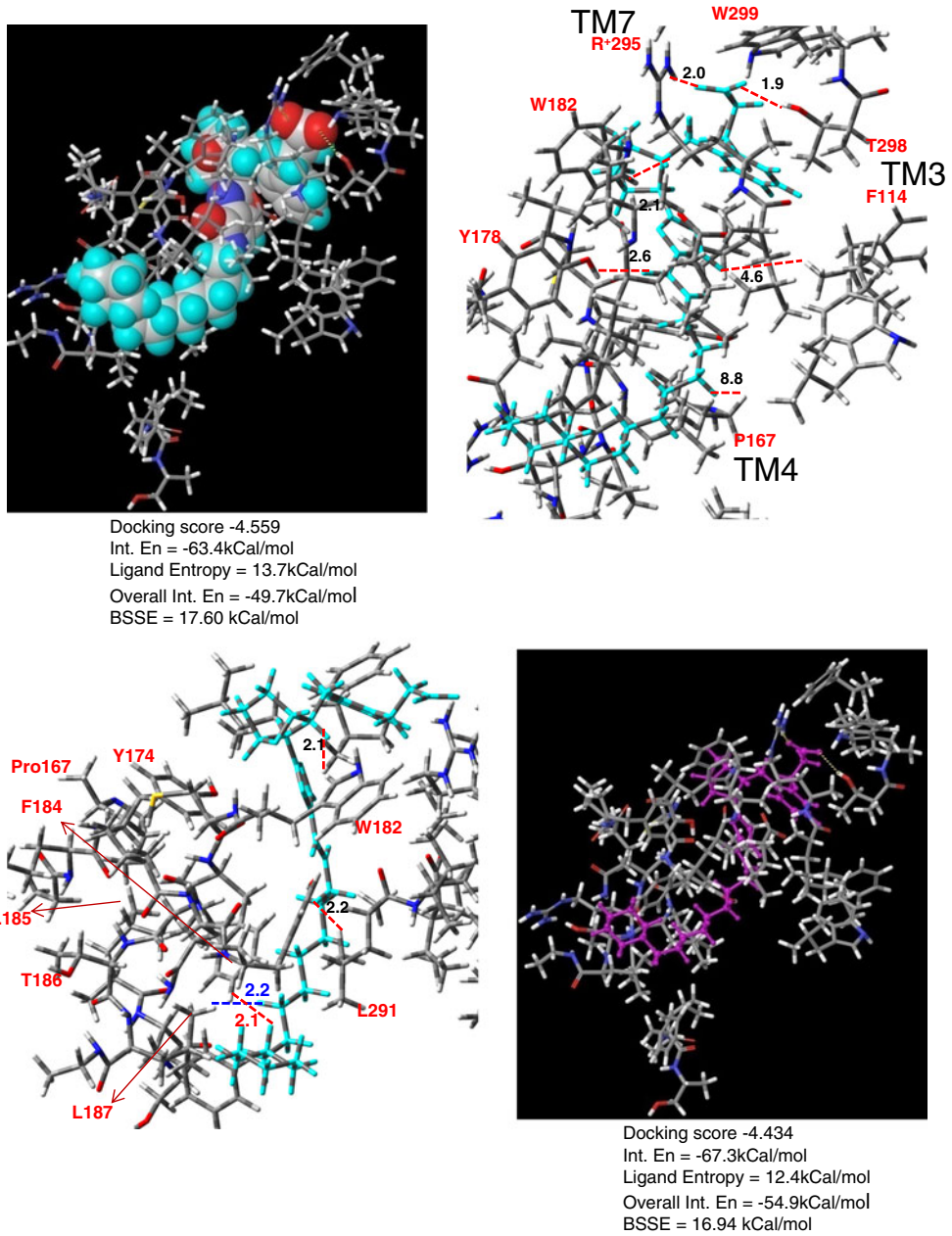

Fig. 7 Best two poses for the flexible ligand docking of antagonist SQ34550 in the TPR. Results of ab initio interaction energy calculations are also shown. Distances are in Å

mation is best suited to the receptor's constrained site, at the expense of minor ligand conformational entropy. The overall interaction energy with the receptor is comparable to that seen for the natural substrate TxA2. The S-shaped conformation of the antagonist shows good binding with the receptor, but it eliminates interactions with TM3 and TM4, implying that these transmembranes are important for receptor activation. Many more TxA2-derived antagonists were also studied. All of them showed similar conformations and hence similar binding modes. Conformational restriction ensures good binding that utilizes electrostatic interactions with $R^{+}295$, but prohibited hydrogen-bonding interactions with F114 and P167. Hydrogen-bonding interactions with Y178/L291 are weakened due to an absence of hydroxyl groups on the prostanoid alkyl chain in most of the antagonists. In other words, the interactions between an antagonist and the receptor only allow the antagonist to bind to the receptor, not to activate it.

After elucidating the mode of action of TPR antagonists, cyclooxygenase 2 (COX 2) inhibitors were studied in order to determine their mode of action. A potent inhibitor of COX, SC558, was selected for this study; its chemical structure and optimized conformations are shown in Fig. 8a. COX inhibitors are not flexible enough to allow many dockable conformations. Most of the inhibitors occur in a compact V form. Similarities and differences between the active sites of the TPR and COX are also shown in Fig. 8b. Similar residues in similar positions, for example $R^{+}295$: $R^{+}513$, $R^{+}173$: $R^{+}120$, and S201: S530, may allow similar substrates to be accepted by both active sites [26]. Therefore, we docked a COX-specific potent drug, SC558, in the active site of COX; the results are shown in Fig. 9. The main binding interactions include the interaction of the sulfonamide group on the drug with Q192 and $H^{+}90$, the interaction of the CF_3 group with $R^{+}120$, and the interaction of the bromophenyl group with W387 and S530. All of the poses show similar binding interactions, as the lack of

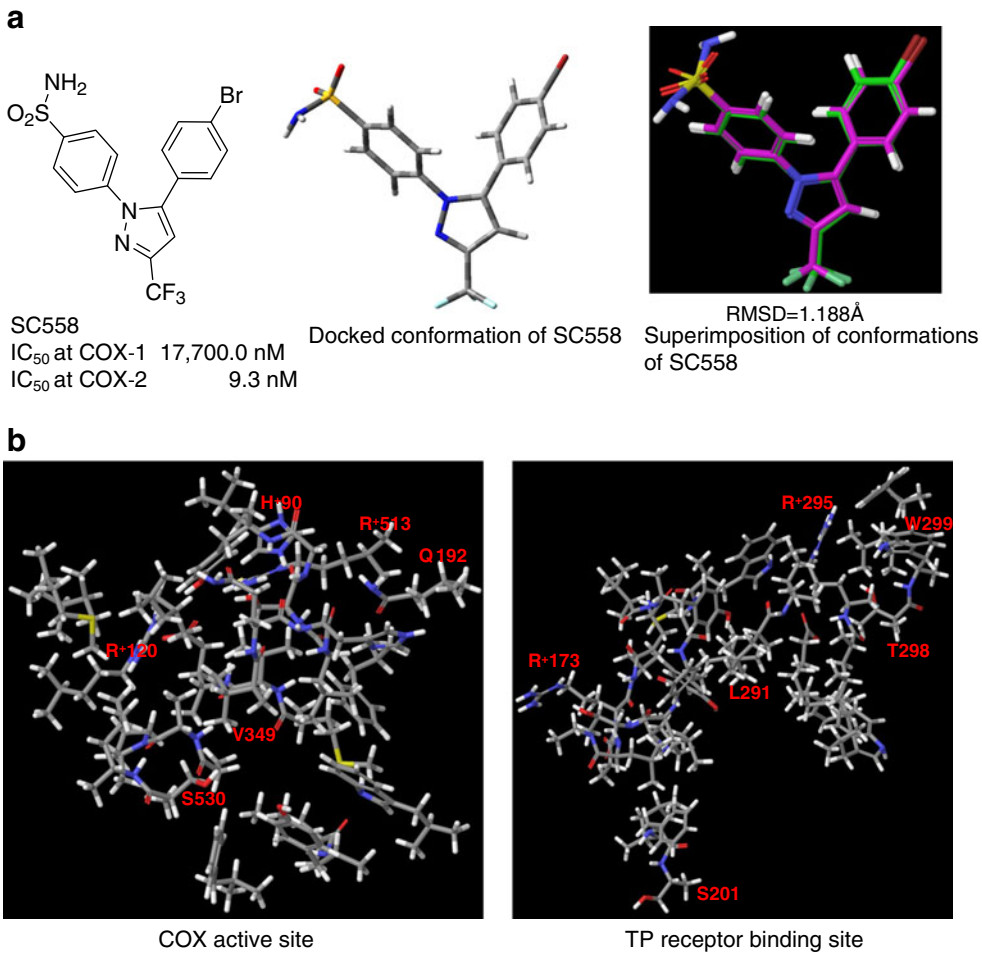

Fig. 8 **a** Conformational mapping for the COX-2 inhibitor SC 558. **b** Comparison of the active sites of COX-2 and the TPR

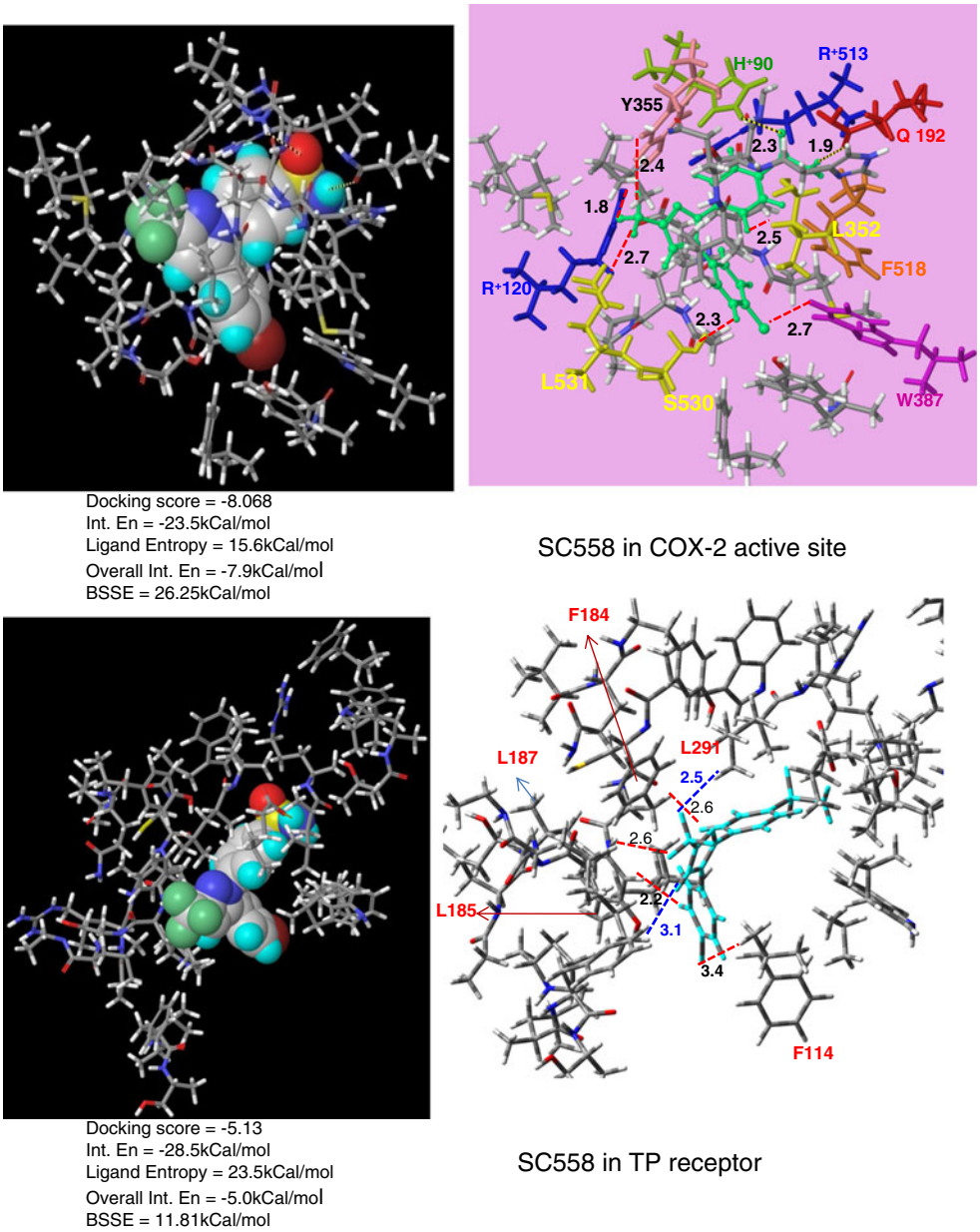

Fig. 9 Best docking score poses for the flexible ligand docking of SC558 in the active site of COX-2 and the TPR binding site. Results of ab initio interaction energy calculations are also shown

flexibility of the compound does not permit it to fit into the active site in various conformations. Mutagenesis results [27, 28] and recent modeling studies [29] have also highlighted the importance of these residues. The overall interaction energy is quite low, as the drug is not in an ionized form and there is no major contribution from electrostatic interactions. The high docking score may be due to the smaller size of the drug.

In order to design a dual inhibitor for TPR and COX, we docked a COX-specific drug in the TPR-binding site, as some sulfonamide derivatives have already been shown to act as TPR antagonists [30, 31]. This docking approach allowed us to identify the modifications that must be made to SC558 to make it a good dual inhibitor. The docking results for SC558 are shown in Fig. 9. This compound, being small in size, is not able to engage with all of the residues needed to bind at the TPR binding site. The main binding residue in the TPR, $R^{+}295$, is still available to interact with the natural substrate. However, it does obstruct TxA2 from interacting with L291, leading to some degree of antagonism at the TPR. Perhaps this is why modern COXIBs are

known to show dual inhibition, leading to synergistic effects.

However, it is important to design balanced dual inhibitors to avoid side effects and to take complete advantage of dual antagonism. Garlic is a well-known herb that possesses many medicinal properties, including antihypertensive and anti-inflammatory properties [32]. It has many constituents, one of which is allicin. We used allicin as our starting point to derive a dual TPR/COX inhibitor. Both of the active sites contain a positive site to anchor the substrate. Therefore, in the first design step, a carboxylic group was introduced at one end of allicin to enhance the binding with the receptor. In the next step, a five-membered ring was introduced at the other end to restrict movement and retain the conformation best suited to docking with the TPR. These design steps are shown in Fig. 10. The docking of designed compound 2 in both receptors is shown in Fig. 11. The change in ligand conformational entropy is negligible for docking in the TPR, which indicates that the designed compound is suitable for antagonizing TPR. The results obtained when the designed compound was docked in the active site of COX are also shown in Fig. 11. The designed compound utilizes electrostatic interactions with $R^{+}120$ in COX-2 and R^{+} 295 in the TPR . It avoids interactions with TM3 and 4 in the TPR, suggesting antagonism. It also presents hydrophobic interactions between the five-membered ring and

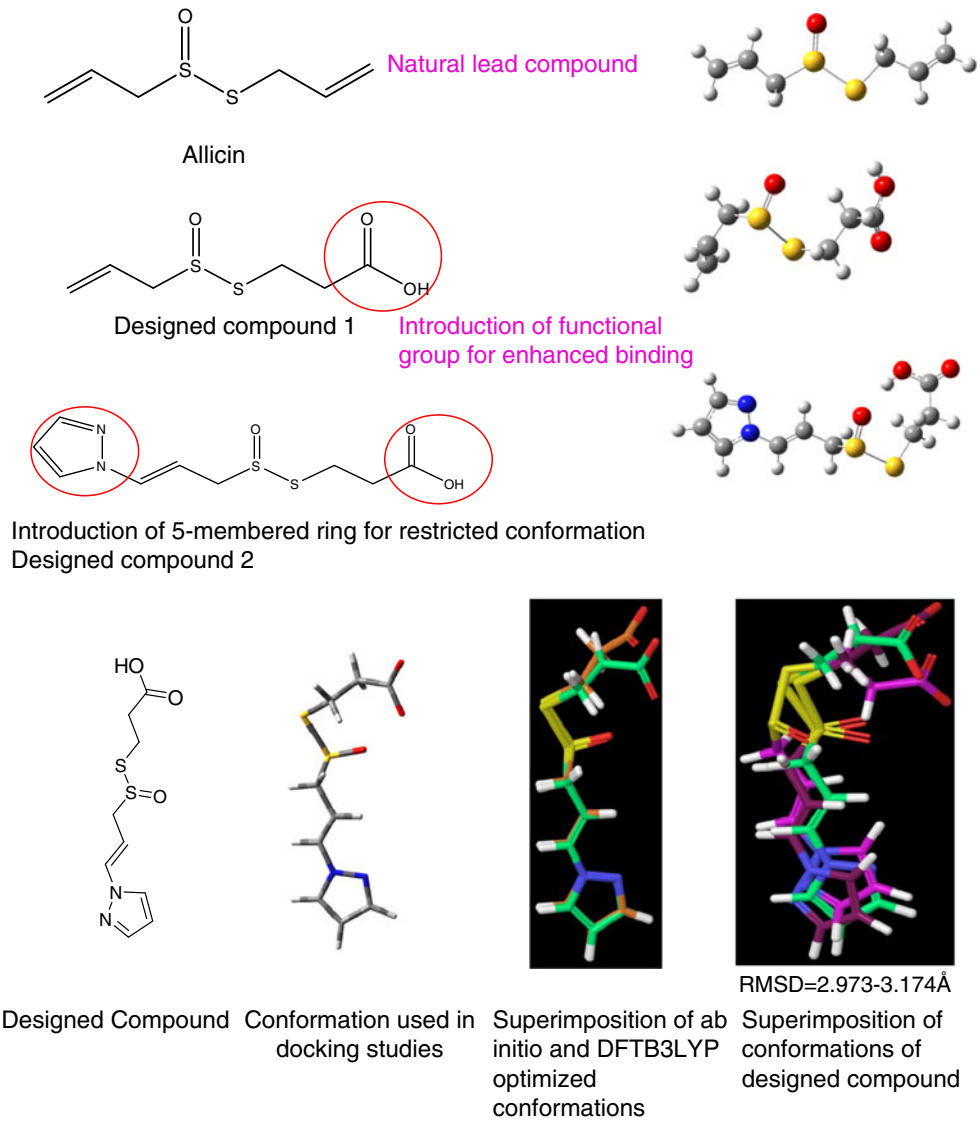

Fig. 10 Chemical structures and optimized conformations of allicin and the designed compounds

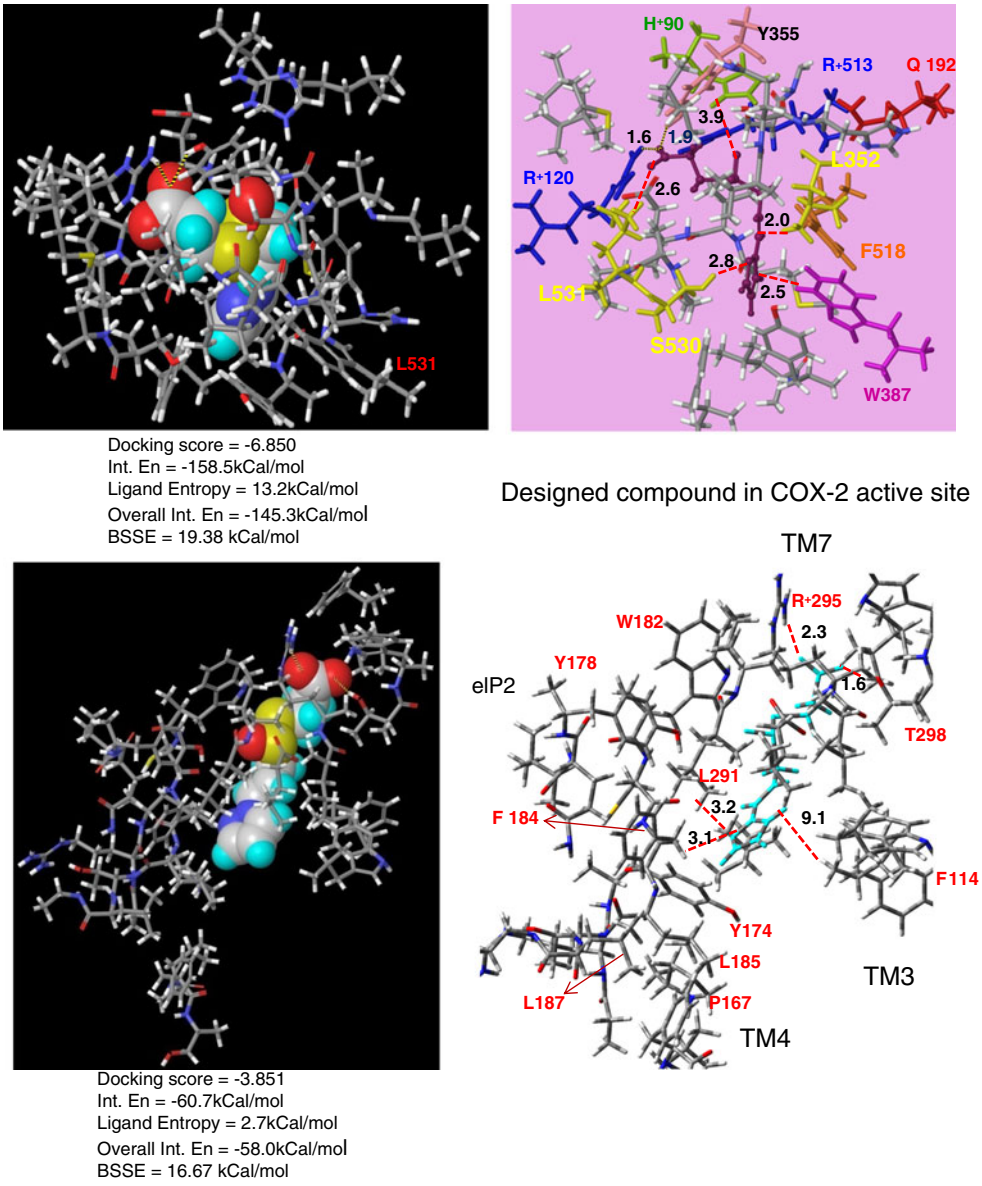

Fig. 11 Best docking score poses for the flexible ligand docking of the designed compound in the active site of COX-2 and the TPR binding site. Results of ab initio interaction energy calculations are also shown

residues in the active site of COX. The sulfone linkage is H-bonded to $H^{+}90$. The designed compound is therefore optimized for dual inhibition due to its enhanced electrostatic interactions with both the receptors. It engages all of the important residues for binding in the TPR (whereas COXIBs—which are also dual inhibitors—leave out $R^{+}295$), making it available to thromboxane. The change in conformational entropy when binding to both receptors is very small, facilitating binding to both.

This designed compound is expected to be a good starting point for the development of a balanced dual TPR/COX inhibitor, and it has the added advantage of being a naturally derived compound.

Concluding remarks

This study utilized a combination of automated flexible ligand docking and ab initio interaction energy calculations to study the modes of action for TxA2 antagonists and COX-2 inhibitors. The binding interactions in both cases were studied in detail at the microscopic level. The resulted increased understanding of these binding interactions led to

the design of a balanced dual inhibitor starting from a natural compound. This compound will fully utilize synergistic effects, and may lead to better anti-inflammatory drugs or better drugs for cardiovascular diseases with fewer side effects.

References

1. Wang LH, Kulmacz RJ (2002) Prostaglandins Other Lipid Mediat 409:68–69
2. Fu JY, Masferrer JL, Seibert K, Raz A, Needleman P (1990) J Biol Chem 265:16737–16740
3. Whittle BJ (2003) Fundam Clin Pharmacol 17:301–313
4. Grosser T et al (2006) J Clin Invest 116:4–15
5. Selg E, Buccellati C, Andersson M, Rovati GE, Ezinga M, Sala A, Larsson AK, Ambrosio E, Lastbom L, Capra V, Dahlen B, Ryrfeldt A, Folco GC, Dahlen SE (2007) Br J Pharmacol 152:1185–1195
6. Rovati GE, Sala A, Capra V, Dahlen SE, Folco G (2010) Trends Pharmacol Sci 31(3):102–107
7. Peng C, Ayala PY, Schlegel HB, Frisch MJ (1996) J Comput Chem 17:49–56
8. Peng C, Schlegel HB (1994) Israel J Chem 33:449–457
9. Petersson GA, Al-Laham MA (1991) J Chem Phys 94:6081–6090
10. Petersson GA, Bennett A, Tensfeldt TG, Al-Laham MA, Shirley WA, Mantzaris J (1988) J Chem Phys 89:2193–2218
11. Liu ECK, Abell LM (2006) Anal Biochem 357:216–224
12. Gierse JK, Hauser SD, Creely DP, Koboldt C, Rangwala SH, Isakson PC, Seibert K (1995) Biochem J 305:479–484
13. Kurumbail RG, Stevens AM, Gierse JK, Mc Donald JJ, Stegeman RA, Pak JY, Gildehaus D, Miyashiro JM, Penning TD, Seibert K, Isakson PC, Stallings WC (1996) Nature 384:644–648
14. Kurumbail RG, Stevens AM, Gierse JK, McDonald JJ, Stegeman RA, Pak JY, Gildehaus D, Miyashiro JM, Penning TD, Seibert K, Isakson PC, Stallings WC (1997) Nature 385:555 (erratum)
15. Hirata M, Hayashi Y, Ushikubi F, Yokota Y, Kageyama R, Nakanishi S, Narumiya S (1991) Nature 349:617–620
16. Kiefer F, Arnold K, Kunzli M, Bordoli L, Schwede T (2009) Nucleic Acids Res 37:D387–D392
17. Kopp J, Schwede T (2004) Nucleic Acids Res 32:D230–D234
18. Friesner RA, Banks JL, Murphy RB, Halgren TA, Klicic JJ, Mainz DT, Repasky MP, Knoll EH, Shaw DE, Shelley M, Perry JK, Francis P, Shenkin PS (2004) J Med Chem 47:1739–1749
19. Halgren TA, Murphy RB, Friesner RA, Beard HS, Frye LL, Polland WJ, Banks JL (2004) J Med Chem 47:1750–1759
20. Friesner RA, Murphy RB, Repasky MP, Frye LL, Greenwood JR, Halgren TA, Sanschagrin PC, Mainz DT (2006) J Med Chem 49:6177–6196
21. Schrödinger LLC (2009) Maestro. Schrödinger LLC, New York
22. So SP, Wu J, Huang G, Huang A, Li D, Ruan KH (2003) J Biol Chem 278(13):10922–10927
23. Yamamoto Y, Kamiya K, Terao S (1993) J Med Chem 36:820–825
24. Nakahata N (2008) Pharmacol Ther 118:18–35
25. Funk CD, Furci L, Moran N, Fitzgerald GA (1993) Mol Pharmacol 44:934–939
26. Selg E, Buccellati C, Andersson M, Rovati GE, Ezinga M, Sala A, Larsson AK, Ambrosio E, Lastbom L, Capra V, Dahlen B, Ryrfeldt A, Folco GC, Dahlen SE (2007) Brit J Pharmacol 152:1185–1195
27. Rowlinson SW, Crews BC, Lanzo CA, Marnett LJ (1999) J Biol Chem 274(33):23305–23310
28. Rowlinson SW, Kiefer JR, Prusakiewicz JJ, Pawlitz JL, Kozak KR, Kalgutkar AS, Stallings WC, Kurumbail RG, Marnett LJ (2003) J Biol Chem 278(46):45763–45769
29. Bouaziz-Terrachet S, Toumi-Maouche A, Maouche B, Tairi-Kellou S (2010) J Mol Model 16:1919–1929
30. Mais DE, Mohamadi F, Dube GP, Kurtz WL, Brune KA, Utterback BG, Spees MM, Jakubowski JA (1991) Eur J Med Chem 26:821–827
31. Gupta AK, Gupta RA, Soni LK, Kaskhedikar SG (2008) Eur J Med Chem 43:1297–1303
32. El-Sabban F (2009) J Chinese Clin Med 41(5):288–294